Inorganic Chemistry

Article

pubs.acs.org/IC

Synthetic Route to Metal Nitrides: High-Pressure Solid-State Metathesis Reaction

Li Lei,*[,†,§] Wenwen Yin,[†] Xiaodong Jiang,[†] Sen Lin,*[,‡] and Duanwei He*[,†,§]

[†]Institute of Atomic and Molecular Physics, Sichuan University, Chengdu 610065, China

[‡]Research Institute of Photocatalysis, Fujian Provincial Key Laboratory of Photocatalysis, State Key Laboratory Breeding Base, Fuzhou University, Fuzhou 350002, China

[§]The Key Laboratory of High Energy Density Physics and Technology (Ministry of Education), Sichuan University, Chengdu 610065, China

Supporting Information

ABSTRACT: We report a general synthetic route to well-crystallized metal nitrides through a high-pressure solid-state metathesis reaction (HPSSM) between boron nitride (BN) and ternary metal oxide $A_xM_yO_z$ (A = alkaline or alkaline-earth metal and M = main group or transition metal). On the basis of the synthetic metal nitrides (Fe_3N, Re_3N, VN, GaN, CrN, and W_xN) and elemental products (graphite, rhenium, indium, and cobalt metals), the HPSSM reaction has been systematically investigated with regard to its general chemical equation, reaction scheme, and characteristics, and its thermodynamic considerations have been explored by density functional theory (DFT) calculations. Our results indicate that pressure plays an important role in the synthesis, which involves an ion-exchange process between boron and the metal ion, opening a new pathway for material synthesis.

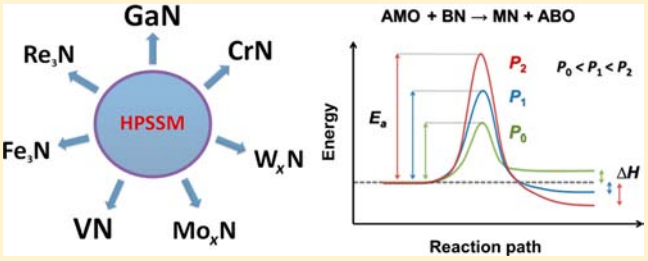

INTRODUCTION

Metal nitrides are important materials for many technological processes, including semiconducting, superconductivity, mechanical, catalytic, optoelectronic, and magnetic applications.[1] However, the preparation of bulk and high-quality metal nitrides is a continuing challenge because the incorporation of nitrogen into a metal lattice is thermodynamically unfavorable. Because nitrogen is very stable and substantially inert, owing to its strong covalent bonds, metal nitride synthesis is more difficult compared to that of the corresponding oxides, halides, and sulfides. Although many technological applications of metal nitrides are expected because of their interesting properties, the preparation of their bulk and stoichiometric crystalline solids has not been well-established. The primary problem is effectively introducing the nitrogen to the metal precursor. In general, metal nitrides are synthesized by reaction of metal or metal oxides with gaseous nitrides, such as ammonia (NH_3) and hydrazine (N_2H_4).[2] However, long durations of the reaction as well as decomposition problems are often encountered in this method. However, alternative synthetic approaches, such as solid-state precursor synthesis and high-pressure synthesis, are effective routes to metal nitrides.

The solid-state metathesis (SSM) reaction, discovered in 1990s and extensively investigated by groups of Kaner,[3] Parkin,[4] and Chen,[5] has been developed as an effective route to many materials such as borides, carbides, and nitrides. Unlike traditional aqueous metathesis (chemical exchange) reactions that result in precipitation or gas release, the combustion-like SSM reaction ignites at a certain temperature and quickly propagates without continuous external heating because it has a very low activation energy, E_a. The SSM reaction for the synthesis of a metal nitride typically involves a metal (M) halide (H) and an alkaline or alkaline-earth (A) nitride (N) compound, and the reaction can described by an ion-exchange scheme: MH + AN → [$M^+ + N^- + AH$] → MN + AH.[6] The SSM reaction often has very high reaction enthalpy, ΔH, leading to combustion-like phenomena. The byproducts of these synthetic routes are often poorly crystalline and have limited scalability (within several micrometers) as a consequence of the very short reaction time (less than a few seconds).[3−6] The common drawbacks of a conventional SSM reaction for the synthesis of high-quality metal nitrides include having a combustible precursor, an uncontrollable reaction process, a small-size, poor crystallinity, and nonstoichiometric product formation.

High-pressure (HP) synthesis based on an elemental direct reaction is an effective route for the discovery of novel metal nitrides.[7] The advantages of high pressure lie in increasing the intimate contact of the surfaces between the two reagents, preventing the thermal decomposition and volatility of the reagents and products at high temperature and varying the oxidation states of the metals with pressure. Over the past 10 years, noble metal nitrides (PtN_2, IrN_2, and OsN_2), Th_3P_4-type

Received: June 12, 2013
Published: November 19, 2013

   dx.doi.org/10.1021/ic4014834 | Inorg. Chem. 2013, 52, 13356−13362

Table 1. Overview of Recently Studied HPSSM Reactions between BN and $A_xM_yO_z$

precursors	P and T conditions	does the reaction occur	reaction products	ref
$LiGaO_2$ + BN	1.0−5.0 GPa, 900−1400 °C	yes	GaN + $LiBO_2$	9
$LiGaO_2$ + BN	15 GPa, 1600 °C	no		this work
$NaGaO_2$ + BN	1.0−5.0 GPa, 1000−1600 °C	yes	GaN + $NaBO_2$	12
$KGaO_2$ + BN	5.0 GPa, 1300−1450 °C	yes	GaN + KBO_2	this work
$NaVO_3$ + BN	5.0 GPa, 1400 °C	yes	VN + $NaBO_2$	this work
$NaVO_2$ + BN	5.0 GPa, 1400 °C	yes	VN + $NaBO_2$	this work
$NaCrO_2$ + BN	0−5.0 GPa, 800−1400 °C	yes	CrN + $NaBO_2$	10
$NaFeO_2$ + BN	5.0 GPa, 1400 °C	yes	Fe_3N + $NaBO_2$ + N_2	this work
$Ca_2Fe_2O_5$ + BN	5.0 GPa, 1400 °C	yes	Fe_3N + $Ca_2B_2O_5$ + N_2	this work
$MgFe_2O_4$ + BN	5.0 GPa, 1400 °C	yes	Fe_3N + MgB_2O_4+ N_2	this work
Na_2CO_3 + BN	5.0 GPa, 1600 °C	yes	graphite + $NaBO_2$ + N_2	this work
Li_2CO_3 + BN	5.0 GPa, 1600 °C	yes	graphite + $LiBO_2$ + N_2	this work
$NaInO_2$ + BN	5.0 GPa, 1400 °C	yes	In + $NaBO_2$ + N_2	this work
$LiInO_2$ + BN	3.5 GPa, 1000 °C	yes	In + $LiBO_2$ + N_2	this work
$NaCoO_2$ + BN	5.0 GPa, 1300−1400 °C	yes	Co + $NaBO_2$ + N_2	this work
$LiNiO_2$ + BN	5.0 GPa, 1400−1500 °C	yes	Ni+ $LiBO_2$ + N_2	this work
Na_2WO_4 + BN	5.0 GPa, 600−2300 °C	yes	W_xN + $NaBO_2$ + N_2	11
Na_2MoO_4 + BN	5.0 GPa, 400−2200 °C	yes	Mo_xN + $NaBO_2$ + N_2	22
K_2OsO_4 + BN	5.0 GPa, 1200 °C	yes	Os + KBO_2 + N_2	22
$NaReO_4$ + BN	5.0 GPa, 1800 °C	yes	Re + $NaBO_2$ + N_2	this work
$NaReO_4$ + BN	14.0 GPa, 1600 °C	yes	Re_3N + Re + $NaBO_2$ + N_2	this work
$LiAlO_2$ + BN	0.5−5.0 GPa, 20−1600 °C	no		13
$NaMnO_2$ + BN	5.0 GPa, 1300−1450 °C	no		this work

metal nitrides (Zr_3N_4 and Hf_3N_4), and rhenium nitrides (Re_2N and Re_3N) have been discovered by the direct elemental reaction between metal elements and nitrogen under high pressure.[7,8] Until now, HP synthesis has still been the only effective method to obtain most of these nitrides. However, the high-pressure elemental direct reaction method has shortcomings, such as a micrometer-scale sample and extreme pressure−temperature conditions.

A novel synthetic route based on a high-pressure solid-state metathesis (HPSSM) reaction was first reported in 2009 by Lei and He on the synthesis of gallium nitride (GaN).[9] Lithium metagallate ($LiGaO_2$) was found to react with boron nitride (BN) at 5.0 GPa and 1200 °C to produce well-crystallized GaN crystals and lithium metaborate ($LiBO_2$).[9] Over subsequent years, some other important metal nitrides (CrN[10] and W_xN[11]) were also successfully synthesized through similar reactions. HPSSM synthesis involves the reactions between new solid-state precursors under high pressure, integrates the merits of the SSM synthesis and HP synthesis, and demonstrates a promising synthetic route to metal nitrides. However, previous studies on the HPSSM reaction have been limited to single-reaction characterization.[9−12] There are still many unanswered questions. For example, why do some reactions occur but others do not, what is the actual role of pressure in the HPSSM reaction, what is the extent to which the HPSSM reaction can apply, and so on.

To obtain further insight into the HPSSM reaction, we present a systematic study on the HPSSM reaction for the synthesis of new metal nitrides (VN, Fe_3N, and Re_3N) and reported metal nitrides (GaN, CrN, and W_xN) as well as newly discovered elemental products (nanosized graphite, plate-like rhenium metal, ball-like indium, and cobalt metal). The reaction products have been characterized by X-ray diffraction (XRD), scanning electron microscopy (SEM), energy-dispersive X-ray analysis (EDX), and Raman spectroscopy. The general chemical equation and reaction scheme are proposed, the synthesis and reaction characteristics (in terms of the reaction precursors and products) are discussed, and thermodynamic considerations by ab initio calculations on pressure-dependent thermodynamic and kinetic parameters, such as activation energy, E_a, and reaction enthalpy, ΔH, were also investigated.

EXPERIMENTAL METHODS

Synthesis, Purification, and Characterization. The high-pressure synthesis experiments were performed on a cubic press, which is now commonly operated in the industrial production of synthetic diamond and cubic BN on a megaton scale. High-pressure experiments below 5 GPa were performed on a first-stage system in the cubic press (DS6 × 14MN, China),[13] and high-pressure experiments above 5 GPa were performed on a second-stage system in the cubic press (DS6 × 8MN, China).[14] Some ternary metal oxides $A_xM_yO_z$ (AMO, A = alkali or alkaline-earth metal and M = main group or transitional metal) were purchased commercially (Alfa Aesar) and some were prepared through a conventional high-temperature solid-state reaction between high-purity metal oxide M_xO_y (Alfa Aesar) and high-purity alkaline or alkaline-earth carbonates A_xCO_3 (Alfa Aesar). The AMO and BN powders, mixed in a desired molar ratio, were used as starting materials for the high-pressure experiments. The starting materials were compacted in advance into a cylindrical pellet (typically 8.0 mm in diameter and 6.0 mm in height), placed in a capsule made of Mo or hexagonal-BN, and then placed in a pyrophyllite high-pressure cell. The sample was first pressurized to a certain pressure, heated to a desired temperature that was maintained for 1−30 min, and then cooled to room temperature.

The metal nitrides products were isolated from the high-pressure quenched samples. The high-pressure recovered products were first ground into powder and washed in distilled water or HCl or HNO_3 to remove the byproduct alkaline or alkaline-earth metal borates and unreacted AMO.

The phase determination and structural characterization of the as-obtained and isolated reaction products were confirmed by powder XRD (λ_{Cu} = 1.54056 Å, Fangyuan DX-2500, China) at 0.03°/s steps over the range of 2θ = 10−100° as well as by home-built confocal micro-Raman spectroscopy. The micro-Raman system is based on a

dx.doi.org/10.1021/ic4014834 | Inorg. Chem. 2013, 52, 13356−13362

triple grating monochromator (Andor Shamrock SR-303i-B, EU) with an attached EMCCD (ANDOR Newton DU970P-UVB, EU), excitation by a solid-state laser at 532 nm (RGB lasersystem, NovaPro 300 mW, Germany) or He−Cr ion laser at 325 nm (Kimmon, 30 mW, Japan), and collection by a 100×, 0.90 NA objective (Olympus, Japan) or a 15× UV-objective (Thorlabs, USA). The size and morphology were investigated by SEM (Hitachi FE-SEM S4800, Japan); the phase homogeneity and compositions were studied by EDX (Hitachi FE-SEM S4800, Japan). Structural refinements were performed with FullProf Suite 1.10 Rietveld refinement program.

Ab Initio Calculations. Periodic DFT was used to provide qualitative confirmation of the experimental observations and to rationalize the effect of pressure that was identified as being correlative with the reactions by means of reaction enthalpy evaluation. All calculations were carried out on the basis of the periodic DFT calculations using the Vienna ab initio simulation package (VASP) with the gradient-corrected PW91 exchange-correction functional.[15] For valence electrons, a plane-wave basis set was employed with a cutoff of 400 eV, and the ionic cores were described with the projector augmented-wave (PAW) method.[16] A 7 × 7 × 7 Monkhorst−Pack *k*-point grid was adopted to sample the Brillouin zone, which is sufficient to obtain accurate results.[17] During the optimization, all of the atoms were allowed to relax using the conjugate-gradient algorithm until the force on each ion was less than 0.01 eV/Å. The optimized lattice constants for the bulk agree very well with the experimental values.

RESULTS AND DISCUSSION

Materials Synthesis via HPSSM Reactions. Table 1 lists our recently studied HPSSM reactions between BN and $A_xM_yO_z$. The facile synthetic route to MN-type trivalent metal nitrides (GaN, VN, and CrN) is depicted in the following general reaction

$$AMO_2 + BN \rightarrow MN + ABO_2 \quad (1)$$

where A is an alkaline metal and M is a trivalent main group or transition metal.

Figure 1A shows a typical SEM image of the isolated GaN crystals prepared by the HPSSM reaction of potassium metagallate ($KGaO_2$) with BN at 5 GPa and 1400 °C. Yellowish GaN grids were readily isolated by washing the reaction products with distilled water to remove the byproduct potassium metaborate (KBO_2) and unreacted $KGaO_2$ (Figure 1A inset). The purified GaN products are hexagonal (space group $P6_3mc$) phase with cell parameters of a = 3.1907(2) Å and c = 5.1906(3) Å (Figure 2A), are well-crystallized, and have a hexagonal cross section (Figure 1A). The typical Ga/N atomic ratio of the obtained crystals is about 53:47 (see Supporting Information Figure S1). We also found that the K-based precursor reaction could give higher yields of GaN crystals than Li- or Na-based precursors.[9,12] In Figure 3A, the Raman bands at 147.6, 535.9, 560.7, and 573.1 cm^{-1} are assigned to the E_2^L, A_1, E_1, and E_2^H modes of hexagonal GaN. The Raman bands at 426 and 670 cm^{-1} (denoted as stars in Figure 3A) correspond to the vacancy-related crystal defects resulting from the synthesis process under pressure.[18]

Similarly, sodium vanadium oxide ($NaVO_2$) reacts with BN at 5 GPa and 1400 °C to produce vanadium nitride (VN). The purified VN products are cubic (space group $Fm\bar{3}m$) phase with a cell parameter of a = 4.1287(2) Å (Figure 2B) and well-crystallized, and they exhibit an octahedral morphology (Figure 1B) without any first-order Raman active mode (Figure 3B) because of their cubic binary rocksalt-type crystal structure.[19] Another example of the reaction in eq 1 is the HPSSM reaction to cubic rocksalt-type CrN (note that this synthesis reaction could also proceed at atmospheric pressure).[10]

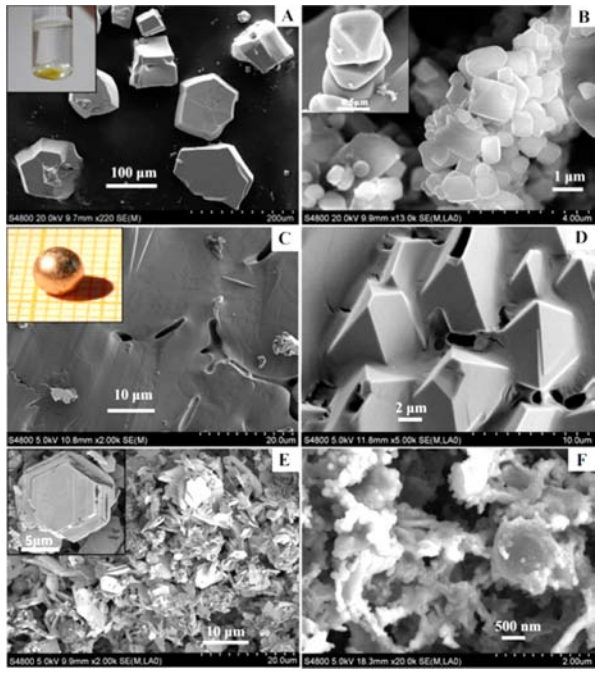

Figure 1. SEM images of the typical purified products resulting from HPSSM reactions between AMO and BN at high pressure and high temperature (HPHT). (A) GaN grids with hexagonal crystalline morphology. The inset shows the yellowish GaN grids isolated by washing with distilled water. (B) Cubic VN grids. The inset shows VN grids with octahedral morphology. (C) Fe_3N sample with nitrogen-degassing-induced cavities in the cross section. The inset is the optical image of the spherical Fe_3N bulk product. (D) Crystalline Re_3N crystals recovered from HPSSM reaction at 14 GPa and 1600 °C. (E) Hexagonal metal Re recovered from 5 GPa and 1800 °C. (F) Graphite particles with a grain size of ∼200 nm recovered from HPSSM reaction at 5 GPa and 1600 °C.

In addition to MN-type metal nitrides, nitrogen-deficient M_xN-type metal nitrides can also be prepared by the HPSSM reaction. A case in point is the synthesis of the surface-hardening material[20] ion nitride (Fe_3N) via the HPSSM reaction between sodium ferrite ($NaFeO_2$) and BN at 5 GPa and 1400 °C. The chemical reaction is depicted as follows

$$3NaFeO_2 + 3BN \rightarrow Fe_3N + N_2 + 3NaBO_2 \quad (2)$$

The isolated product is a sintered spherical body of ∼4 mm in diameter (Figure 1C, inset). Note that the sample chamber is only ∼8 mm in diameter. The SEM image in Figure 1C demonstrates that nitrogen-degassing induced cavities in the cross section of the as-synthesized products. EDX indicates that the x value of the as-synthesized Fe_xN is very close to 3.0 (see Supporting Information Figure S2). The powder XRD pattern in the Figure 2C reveals that the metallic ball-like product is the hexagonal ε-Fe_3N (space group $P312$) with cell parameters of a = 4.7410(2) Å and c = 4.3862(2) Å. Group theory shows that the hexagonal Fe_3N should have 11 Raman active modes, 3A1 + 8E. However, we could not detect any Raman band using the 532 nm Raman laser. If the laser power on the sample is too high, such as >20 mW, then the Fe_3N will be decomposed and oxidized, and hematite Fe_2O_3 would be detected. By using the 325 nm UV laser, only one Raman band at 338 cm^{-1} was observed, which can be assigned to the Fe−N bond vibration.[21]

It was found that not only alkaline metal oxide but also alkaline-earth metal oxide could trigger the HPSSM reaction to

dx.doi.org/10.1021/ic4014834 | Inorg. Chem. 2013, 52, 13356−13362

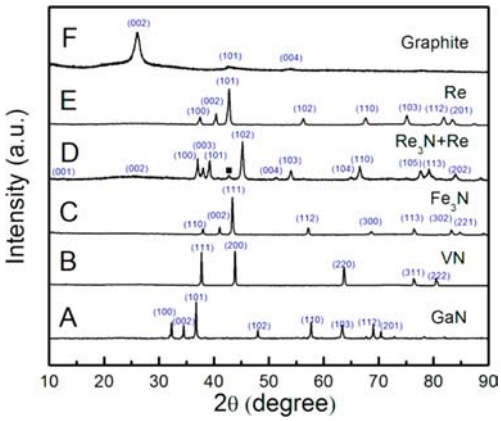

Figure 2. Powder XRD patterns of the synthetic products resulting from HPSSM reactions between AMO and BN at HPHT. (A) Hexagonal GaN (space group $P6_3mc$, a = 3.1907(2) Å, and c = 5.1906(3) Å). (B) Cubic VN (space group $Fm\bar{3}m$, a = 4.1287(2) Å). (C) Hexagonal Fe_3N (space group $P312$, a = 4.7410(2) Å,and c = 4.3862(2) Å). (D) Hexagonal Re_3N (space group $P\bar{6}m2$, a = 2.8110(3) Å, and c = 7.1394(4) Å) and hexagonal Re (space group $P6_3/mmc$, denoted as square) recovered from HPSSM reaction at 14 GPa and 1600 °C. (E) Hexagonal Re (space group $P6_3/mmc$, a = 2.7663(2) Å, and c = 4.4607(3) Å) recovered from HPSSM reaction at 5 GPa and 1800 °C. (F) Hexagonal graphite (space group $P6_3/mmc$, a = 2.5714(18) Å, and c = 6.8382(27) Å) with broad diffraction peaks induced by the nanosized effect. X-ray diffraction patterns of products are indexed with Miller indices.

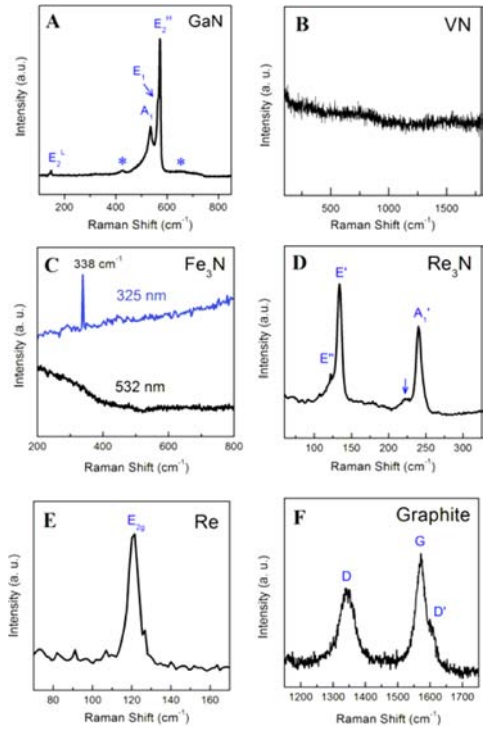

Figure 3. Raman spectra of the synthetic products resulting from HPSSM reactions between AMO and BN. (A) Hexagonal GaN. (B) Cubic VN. (C) Hexagonal Fe_3N. (D) Hexagonal Re_3N. (E) Hexagonal metal Re. (F) Nanosized hexagonal graphite. The Raman active modes are indexed. The 532 and 325 nm laser power is ~10 and ~15 mW, respectively.

Fe_3N. For example, calcium ferrite ($Ca_2Fe_2O_5$) and magnesium ferrite ($MgFe_2O_4$) are able to react with BN to form similar Fe_3N products under identical synthetic conditions. It is known that the atmospheric-pressure melting points of $NaFeO_2$, $Ca_2Fe_2O_5$, and $MgFe_2O_4$ are 1350, 1440, and 1710 °C, respectively. The melting point will significantly increase with pressure. Therefore, the high-pressure melting points of these metal-oxide precursors (and BN) will be higher than the synthetic temperatures (typical 1400 °C). The initial HPSSM reaction for the synthesis of Fe_3N occurs at the interface between the two solid-state precursors, and the metathesis reaction products (Fe_3N and $NaBO_2$) will be distributed in the whole sample chamber in the form of tiny particles. However, because the reaction temperature (1400 °C) is much higher than the melting point of the byproduct $NaBO_2$ (970 °C at atmospheric pressure), $NaBO_2$ will be in the molten state and will very easily gather together like a kind of solvent, and the Fe_3N products in the $NaBO_2$ melt will tend to gather into a ball (Figure 1C, inset) because of the effect of the surface energy. Further studies are currently in progress to explore the detailed properties of the newly prepared Fe_3N products.

Another case in point is the synthesis of novel hexagonal Re_3N via the HPSSM reaction between sodium perrhenate ($NaReO_4$) and BN at 14 GPa and 1600 °C. The hexagonal Re_3N is a novel heavy-metal nitride material recently discovered by the elemental direct reaction at 13−16 GPa in diamond anvil cell (DAC) experiments.[8] In this work, better-crystallized and bulk Re_3N (Figure 1D) was able to be prepared by the HPSSM reaction under similar synthetic conditions. Figure 2D shows the powder XRD pattern for the isolated Re_3N products. Hexagonal Re_3N (space group $P\bar{6}m2$, a = 2.8110(3) Å, and c = 7.1394(4) Å) is the major phase in the isolated reaction products, with a small amount impurity of hexagonal elemental metal rhenium. Figure 3D is the Raman spectrum of the as-prepared Re_3N. The Raman bands at 122, 134, and 240 cm^{-1} are assigned to the hexagonal Re_3N Raman modes E″, E′, and A_1', respectively. The Re_3N Raman mode (E″) at 122 cm^{-1} is very close to the only Raman mode (E_{2g}) of pure rhenium at 121 cm^{-1} (Figure 3E) because the Re_3N structural mode is built on the hexagonally close-packed layers of rhenium atoms in an ABB stacking sequence.[8] The broad Raman peak at 223 cm^{-1} (labeled with an arrow) likely results from the N-related local vibrational mode. It was also found that low pressure (such as 5 GPa) results in phase-pure Re metal (Figures 1E and 2E; see also Supporting Information Figure S3) instead of Re_3N. Because the rhenium metal is a well-known refractory material with an ultrahigh melting point (>3000 °C), it was not expected that the hexagonal rhenium (space group $P6_3/mmc$, a = 2.7663(2) Å, and c = 4.4607(3) Å) would crystallize well (Figure 1E) when it is far below its melting point under high pressure (5 GPa and 1800 °C).

Generally, high temperature brings about the decomposition or degassing of metal nitride; however, high pressure may delay the onset of these processes. The degassing reaction under high pressure is a useful method for the preparation of variable-nitrogen-content metal nitrides, and metal nitrides prepared at higher pressure commonly have higher nitrogen content. A good case in point is the synthesis of W_xN through the HPSSM reaction between sodium tungstate (Na_2WO_4) and BN. The formation of hexagonal WN and cubic $W_{3/4}N$ is due to the nitrogen-degassing process of hexagonal $W_{2/3}N$ under high pressure.[11] In the case of the Re−N system, however, the elemental Re, Re_3N, and Re_2N[8] are formed at 5, 14, and 20 GPa, respectively. The HPSSM reaction leads to only elemental Re metal because of the lack of enough applied pressure. From

dx.doi.org/10.1021/ic4014834 | Inorg. Chem. 2013, 52, 13356−13362

Table 1, in addition to the Re−N system, HPSSM reactions also resulted in corresponding elemental metals (such as In, Co, Ni, and Os[22]) instead of the desired metal nitride products because of the insufficient applied pressure. For example, the HPSSM reaction between sodium indate ($NaInO_2$) and BN occurs at 5 GPa and 1400 °C, and the isolated reaction product is ball-like metal indium (see Supporting Information Figure S4). The reaction can be depicted as follows

$$NaInO_2 + BN \rightarrow In + 0.5N_2 + NaBO_2 \quad (3)$$

According to the experimentally reported pressure−temperature phase diagram,[23] indium nitride (InN) is unable to form at 5 GPa and 1400 °C, and it will decompose into elemental indium and nitrogen at 5 GPa and above 800 °C. Even if the ion-exchange process between boron and indium does occur and $NaBO_2$ is able to form, InN still fails to come into being under these synthetic conditions (5 GPa and 1400 °C) because of the nature of decomposition. Therefore, elemental indium was obtained in the final isolated products.

From Table 1, it is very interesting that lithium carbonate (Li_2CO_3) or sodium carbonate (Na_2CO_3) is able to react with BN to form graphite and the corresponding metal borate at 5 GPa and 1600 °C (see Supporting Information Figure S5). From Figure 1F, the grain size of the isolated graphite is ∼200 nm, and the nanosized particles of graphite are very easy to aggregate. The broad XRD peaks (Figure 2F), the broad fingerprint (G, D, and D′ bands) Raman modes (Figure 3F), and EDX analysis (see Supporting Information Figure S6) indicate that the isolated reaction products are nanosized hexagonal graphite (space group $P6_3/mmc$, a = 2.5714(18) Å, and c = 6.8382(27) Å). It was expected that carbon nitrides (C_3N_4) or nanosized diamonds could be synthesized under elevated pressure and temperature conditions. It was suggested that not only metal nitride but also nonmetallic nitride might be prepared by the HPSSM reaction, which is the essential extension of the HPSSM reaction.

General Chemical Equation and Reaction Scheme. From Table 1, the HPSSM reactions result in a series of important metal nitrides, such as GaN, CrN,[10] VN, Fe_3N, Mo_xN,[22] W_xN,[11] and Re_3N. The general equation for the HPSSM reaction is depicted in eq 4.

$$A_xM_yO_z + (2z - ax)/3\ BN \rightarrow y/w\ M_wN + 0.5((2z - ax)/3 - y/w)\ N_2 + A_xB_{(2z-ax)/3}O_z \quad (4)$$

where a = 1 when A is an alkaline metal and a = 2 when A is an alkaline-earth metal.

Metal A indicates the alkaline (Li, Na, and K) or alkaline-earth metal (Mg and Ca), and metal M represents main group (Ga and In) or transition metals (Fe, V, Cr, W, Mo, and Re). The HPSSM reaction mechanism could be regarded as a two-stage process. The first-stage of the reaction is the ion exchange behavior between B and M and at the same time the formation of the stable salt ABO; the second-stage of the reaction is the combination of M and N followed by the formation of the metal nitride.

$$AMO + BN \rightarrow [M^+ + N^- + ABO] \rightarrow MN + ABO \quad (5)$$

$$AMO + BN \rightarrow [M^+ + N^- + ABO] \rightarrow M + 0.5N_2 + ABO \quad (6)$$

If the applied pressure is high enough, then the target metal nitride MN could form, as illustrated in eq 5; if the applied pressure is insufficient, then the metal nitride is unable to be produced, but the elemental metal and nitrogen are formed, as described in eq 6. In the case of Fe_3N, for example, the actual processes may lie somewhere between the former and the latter. Our experimental observations also indicate that the necessary conditions for the first-stage ion-exchange process and the formation of stable byproduct ABO are often lower than the synthetic conditions of the second-stage MN combination process.

Reaction Characteristics. With respect to precursors, in the conventional SSM reaction, the combustible alkaline or alkaline-earth metal nitride serves as the precursor of the metal source, and the metal halides are used as the nitrogen precursors; in the novel HPSSM reaction, the solid-state ternary metal oxides AMO are used as the precursors for metal sources, and BN serves as the nitrogen source. Metal oxides are important precursors in the synthesis of metal nitrides because they are easy to prepare, inexpensive, and diverse. The nitridation of a metal-oxide precursor is a thermodynamically favored process under high-pressure and high-temperature conditions. Ternary metal oxide AMO exhibits various high-pressure polymorphs or modifications under high pressure.[13,14,19,24] We found that the polymorphism of the precursor under high pressure may not affect the reaction process, the initial valence state may not change the chemical-exchange process in the reaction, and the occurrence of the reaction is independent of the melting point of the precursors (see Supporting Information Table S1). In some HPSSM reactions, the typical reaction temperature (1000−1400 °C) is not higher than the melting points of BN (>3000 °C) and some AMO precursors such as $LiGaO_2$ (>1600 °C), $Ca_2Fe_2O_5$ (>1400 °C), and $MgFe_2O_4$ (>1700 °C). Because the ternary metal oxides have higher melting temperatures at high pressure, the HPSSM reactions occur between two solid-state precursors.

In the HPSSM, BN (either hexagonal or cubic polymorph) serves as the nitrogen source. Besides providing high nitrogen potential for the synthetic reaction, the use of the BN precursor leads to thermodynamically favored byproduct metal borates (e.g., $LiBO_2$ and $NaBO_2$). Because of their relatively low melting points (<1000 °C) (see Supporting Information Table S2), metal borates would melt under the synthetic conditions (typically 5 GPa and 1400 °C).[24] The molten borate served as a solution that could speed the diffusion and enhance the nitride-formation process. In addition, metal borates are readily washed by water, which makes the purification of the metal nitride very easy. One of the common points between SSM and HPSSM is that both are driven by the formation of stable salt byproducts, which are then washed away to isolate the product of interest. Another common point is that both SSM and HPSSM reaction precursors involve, without exception, the alkaline or alkaline-earth metal. It was expected that the alkaline or alkaline-earth metal may play an essential role in the metathesis reaction, which was made clear by the present work.

High pressure could not only increase the intimate contact of the surfaces between the two precursors but also effectively prevent thermal decomposition and volatility of the oxide precursors and the nitride products at high temperature. Both

the conventional SSM and HPSSM reactions could result in elemental metal because of decomposition or the nitrogen-degassing reaction. However, the effect of high pressure in the HPSSM reaction could prevent nitrogen from degassing out of the sample to some extent. The nonstoichiometric (sub-stoichiometric) product is formed partly because of the insufficient applied pressure (the nitrogen content of a metal nitride always increases with applied pressure). The HPSSM synthesis gives higher and better yields of metal nitride as compared with SSM synthesis and HP synthesis. The high-pressure annealed metal nitrides often have a simple cubic rocksalt-type (VN and CrN) or hexagonal (GaN, ε-Fe_3N, and Re_3N) crystal structure. The striking feature of the synthetic route is that the new solid-state precursor reaction proceeds via ion exchange between boron and the metal ion, in which pressure plays an essential role. For further insight into the reaction, thermodynamic considerations with the aid of density functional theory (DFT) calculations were also carried out in this work.

Thermodynamic Considerations. The effect of pressure on the HPSSM reaction process was investigated by DFT calculations. For simplicity, six typical reactions in eq 1 were selected (details are given in the caption of Figure 4). The

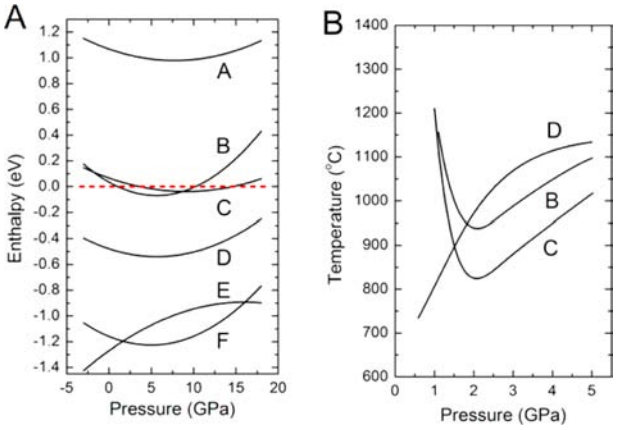

Figure 4. (A) Pressure dependence of the calculated reaction enthalpy using DFT and (B) experimental formation boundary for the synthesized metal nitrides. Solid lines represent the ion-exchange reactions (a) $LiAlO_2 + BN \rightleftharpoons AlN + LiBO_2$, (b) $NaGaO_2 + BN \rightleftharpoons GaN + NaBO_2$, (c) $LiGaO_2 + BN \rightleftharpoons GaN + LiBO_2$, (d) $NaCrO_2 + BN \rightleftharpoons CrN + NaBO_2$, (e) $NaCoO_2 + BN \rightleftharpoons Co + 1/2N_2 + NaBO_2$, and (f) $NaCoO_2 + BN \rightleftharpoons CoN + NaBO_2$. The dashed line denotes zero enthalpy.

reaction enthalpies were computed as a function of the applied pressure. All of the calculations describe the same facts as the experiments,[7,12−14] suggesting that pressure plays an important role in the HPSSM reaction. The enthalpy of the reaction of $LiAlO_2$ with BN (Figure 4A) was found to be positive over the entire pressure range, indicating that the formation of AlN is thermodynamically unfavorable. For the reactions between $AGaO_2$ (A = Li and Na) and BN, the simulated curves of the reaction enthalpy are below zero at medium pressure (~5 GPa), and the synthesis reactions cannot occur at lower (<1 GPa) or higher pressures (>15 GPa). In the case of the reaction of $NaCrO_2$ with BN, the enthalpy has a negative value over the entire calculated pressure range, suggesting that reaction d is thermodynamically favorable at atmospheric pressure or at high pressures. For the reaction between $NaCoO_2$ and BN, although reactions e and f have negative reaction enthalpies over the entire calculated pressure range, reaction e has a lower enthalpy value at low pressure compared with reaction f, implying that the reaction e will be the thermodynamically favorable at atmospheric pressure, which explains the chemical reaction (eq 3) and the appearance of the elemental cobalt in the final reaction products.

The data shown in Figure 4A clearly indicates that pressure may reduce the reaction enthalpy, ΔH, in a reaction between AMO and BN. The positive-slope formation boundary in Figure 4B implies that the reaction activation energy, E_a, increases with applied pressure and the negative slope below 2 GPa implies the signature of a thermodynamically unfavorable reaction at lower pressure. In the case of the HPSSM reaction between AMO_2 and BN, the pressure of ~5 GPa is the optimal parameter in the dimension of pressure. Figure 5 demonstrates

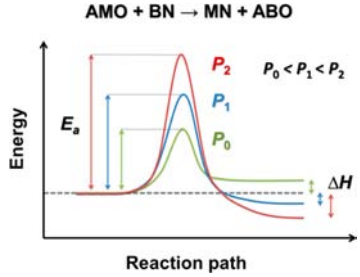

Figure 5. Schematic potential-energy diagram showing the effect of pressure in the reaction between AMO and BN. Pressure, P, opens different reaction pathways with lower reaction enthalpy, ΔH, and higher activation energy, E_a.

the effect of pressure on the HPSSM reaction between AMO with BN. The presence of pressure (P) opens a reaction pathway with a lower reaction enthalpy, ΔH, and a higher activation energy, E_a. The E_a of the HPSSM reaction increases with applied pressure, and it is much higher than that of the SSM reaction. Therefore, the SSM reactions generally occur upon mixing, grinding, or brief contact with a heated filament, whereas the HPSSM reactions could occur by continuous heating above 1000 °C under high pressure. The pressure-driven ΔH of the HPSSM reaction is much lower than that of the SSM reaction, so the SSM reactions are always combustion-like and uncontrollable, whereas the HPSSM reactions are relatively mild without a sharp exotherm. The HPSSM reaction has been demonstrated to be a practical and effective method for synthesizing metal nitrides. Pressure plays an important role in the synthesis reaction. The advantage of using high pressure is generally considered to be a result of increasing the intimate surface contact between two reagents, preventing thermal decomposition and volatility of the reagents and metal nitrides at high temperature and varying the oxidation states of the metals with pressure. Here, we demonstrated that pressure could open an ion-exchange pathway for synthesis. It is expected that many more metal nitrides, nonmetal nitrides, or even elemental products could be synthesized through the presented HPSSM reactions in the future. It is also possible to synthesize other novel materials via the proposed high-pressure metathesis synthetic strategy, which could be significant in the development of material synthesis under high pressure.

dx.doi.org/10.1021/ic4014834 | Inorg. Chem. 2013, 52, 13356−13362

CONCLUSIONS

We report a general and practical strategy for the preparation of metal nitrides by a new HPSSM reaction between ternary metal oxides $A_xM_yO_z$ and BN. The final metal nitride products were phase-pure, near-stoichiometric, well-crystallized, and in bulk form. The general equation for the reaction as well as its common characteristics, reaction scheme, and mechanisms have been discussed. The striking feature of this synthetic route is that it is based on a solid-state reaction that proceeds via ion exchange between boron and a metal ion, where pressure play an essential role in the reaction process. Our results strongly suggest that the meththesis reaction under high compression could open a new pathway to material synthesis.

ASSOCIATED CONTENT

Supporting Information

SEM image, EDX spectra, and analysis of synthetic GaN and Fe_3N crystals as well as rhenium metal. Optical image, SEM image, and XRD pattern of synthetic indium metal. XRD pattern of products (graphite and $NaBO_2$) thought the HPSSM reaction between Na_2CO_3 and BN. Atmospheric-pressure melting points of precursors ($A_xM_yO_z$ and BN) byproduct metal borate ABO_2 and HPSSM reaction temperatures of precursors. This material is available free of charge via the Internet at http://pubs.acs.org.

AUTHOR INFORMATION

Corresponding Authors

* E-mail: lei@scu.edu.cn (L.L.).
*E-mail: slin@fzu.edu.cn (S.L.).
*E-mail: duanweihe@scu.edu.cn (D.H.).

Author Contributions

L.L. and D.H. designed and planned the study. L.L., D.H., and S.L. wrote the manuscript. W.Y. and X.J. conducted the experiments (supervised by L.L.). S.L. performed the calculations.

Notes

The authors declare no competing financial interest.

ACKNOWLEDGMENTS

This work was supported by the China 973 Program (grant no. 2011CB808200), the National Natural Science Foundation of China (grant nos. 11027405, 21203026, and 21301122), and Sichuan University. We thank Jianyi Ma for helpful discussions.

REFERENCES

(1) (a) Morkoc, H.; Mohammad, S. N. *Science* **1995**, *267*, 51. (b) Papaconstantopoulos, D. A.; Pickett, W. E.; Klein, B. M.; Boyer, L. L. *Phys. Rev. B* **1985**, *31*, 752. (c) Guo, K.; Rau, D.; Toffoletti, L.; Müller, C.; Burkhardt, U.; Schnelle, W.; Niewa, R.; Schwarz, U. *Chem. Mater.* **2012**, *24*, 4600. (d) Kroll, P.; Schroter, T.; Peters, M. *Angew. Chem., Int. Ed.* **2005**, *44*, 4249.

(2) Jacob, T. K.; Verma, R.; Mallya, M. R. *J. Mater. Sci.* **2002**, *37*, 4465.

(3) (a) Gillan, G. E.; Kaner, B. R. *Chem. Mater.* **1996**, *8*, 333. (b) Wiley, B. J.; Kaner, B. R. *Science* **1992**, *255*, 1093. (c) Wallance, H. C.; Kim, S.; Rose, A. G.; Rao, L.; Heath, R. J.; Nicol, M.; Kaner, B. R. *Appl. Phys. Lett.* **1998**, *72*, 596.

(4) (a) Parkin, I. P. *Chem. Soc. Rev.* **1996**, *25*, 199. (b) Hector, A. L.; Parkin, I. P. *Chem. Mater.* **1995**, *7*, 1728. (c) Parkin, I. P.; Nartowski, A. M. *Polyhedron* **1998**, *17*, 2617.

(5) (a) Zhao, H.; Lei, M.; Yang, X.; Jian, J.; Chen, X. *J. Am. Chem. Soc.* **2005**, *127*, 15722. (b) Song, B.; Chen, X.; Han, J.; Jian, J.; Wang, W.; Zuo, H.; Zhang, X.; Meng, S. *Inorg. Chem.* **2009**, *48*, 10519. (c) Song, B.; Jian, J.; Wang, G.; Lei, M.; Xu, Y.; Chen, X. *Chem. Mater.* **2007**, *19*, 1497.

(6) (a) Gibson, K.; Ströbele, M.; Blaschkowski, B.; Glaser, J.; Weisser, M.; Srinivasan, R.; Kolb, J. H.; Meyer, J. H. *Z. Anorg. Allg. Chem.* **2003**, *629*, 1863. (b) Meyer, H. *Dalton Trans.* **2010**, *39*, 5973.

(7) (a) McMilian, P. F. *Nat. Mater.* **2002**, *1*, 19. (b) Gregoryanz, E.; Sanloup, C.; Somayazulu, M.; Badro, J.; Fiquet, G.; Mao, H.; Hemley, J. R. *Nat. Mater.* **2004**, *3*, 294. (c) Crowhurst, C. J.; Goncharov, F. A; Sadigh, B.; Evans, L. C.; Morrall, G. P.; Ferreira, L. J.; Nelson, J. A. *Science* **2006**, *311*, 1275. (d) Zerr, A.; Miehe, G.; Riedel, R. *Nat. Mater.* **2003**, *2*, 185. (e) Zerr, A.; Riedel, R.; Sekine, T.; Lowther, E. J.; Ching, W.; Tanaka, I. *Adv. Mater.* **2006**, *18*, 2933. (f) Horvath-Bordon, E.; Riedel, R.; Zerr, A.; McMillan, F. P.; Auffermann, G.; Prots, Y.; Bronger, W.; Kniep, R.; Kroll, P. *Chem. Soc. Rev.* **2006**, *35*, 987. (g) Young, F. A.; Sanloup, C.; Gregoryanz, E.; Scandolo, S.; Hemley, J. R.; Mao, H. *Phys. Rev. Lett.* **2006**, *96*, 155501. (h) Kawamura, F.; Yusa, H.; Taniguchi, T. *Appl. Phys. Lett.* **2012**, *100*, 251910.

(8) (a) Friedrich, A.; Winkler, B.; Bayarjargal, L.; Morgenroth, W.; Juarez-Arellano, A. E.; Milman, V.; Refson, K.; Kunz, M.; Chen, K. *Phys. Rev. Lett.* **2010**, *105*, 085504. (b) Friedrich, A.; Winkler, B.; Refson, K.; Milman, V. *Phys. Rev. B* **2010**, *82*, 224106.

(9) Lei, L.; He, D. *Cryst. Growth Des.* **2009**, *9*, 1264.

(10) Chen, M.; Wang, S.; Zhang, J.; He, D.; Zhao, Y. *Chem.—Eur. J.* **2012**, *18*, 15459.

(11) Wang, S.; Yu, X.; Lin, Z.; Zhang, R.; He, D.; Qin, J.; Zhu, J.; Han, J.; Wang, L.; Mao, H.; Zhang, J.; Zhao, Y. *Chem. Mater.* **2012**, *24*, 3023.

(12) Ma, H.; He, D.; Lei, L.; Wang, S.; Chen, Y.; Wang, H. *J. Alloys Compd.* **2011**, *509*, 124.

(13) Lei, L.; He, D.; Zou, Y.; Zhang, W.; Wang, Z.; Jiang, M.; Du, M. *J. Solid State Chem.* **2008**, *181*, 1810.

(14) (a) Lei, L.; Irifune, T.; Shinmei, T.; Ohfuji, H.; Fang, L. *J. Appl. Phys.* **2010**, *108*, 083531. (b) Xu, C.; He, D.; Wang, H.; Guan, J.; Liu, C.; Peng, F.; Wang, W.; Kou, Z.; He, Kai.; Yan, X.; Bi, Y.; Liu, L.; Li, F.; Hui, B. *Int. J. Refract. Met. Hard Mater.* **2013**, *36*, 232.

(15) (a) Kresse, G.; Hafner, J. *Phys. Rev. B* **1993**, *47*, 558. (b) Kresse, G.; Furthmuller, J. *Phys. Rev. B* **1996**, *54*, 11169. (c) Kresse, G.; Furthmuller. *Comput. Mater. Sci.* **1996**, *6*, 15. (d) Perdew, J. P.; Chevary, J. A.; Vosko, S. H.; Jackson, K. A.; Pederson, M. R.; Singh, D. J.; Fiolhais, C. *Phys. Rev. B* **1992**, *46*, 6671.

(16) (a) Blochl, P. *Phys. Rev. B* **1994**, *50*, 17953. (b) Kresse, G.; Joubert, D. *Phys. Rev. B* **1999**, *59*, 1758.

(17) (a) Methfessel, M.; Paxton, A. T. *Phys. Rev. B* **1989**, *40*, 3616. (b) Monkhorst, H. J.; Pack, J. D. *Phys. Rev. B* **1976**, *13*, 5188.

(18) Wang, S. Ph.D. Thesis, Sichuan University, China, 2013.

(19) (a) Lei, L.; Ohfuji, H.; Irifune, T.; Qin, J.; Zhang, X.; Shinmei, T. *J. Appl. Phys.* **2012**, *112*, 043501. (b) Lei, L.; Ohfuji, H.; Qin, J.; Zhang, X.; Wang, F.; Irifune, T. *Solid State Commun.* **2013**, *164*, 6.

(20) Niewa, R.; Rau, D.; Wosylus, A.; Meier, K.; Hanfland, M.; Wessel, M.; Dronskowski, R.; Dzivenko, A. D.; Riedel, R.; Schwarz, U. *Chem. Mater.* **2009**, *21*, 392.

(21) (a) Franzen, S.; Boxer, G. S.; Dyer, B. R.; Woodruff, H. W. *J. Phys. Chem. B* **2000**, *104*, 10359. (b) Schelvis, P. M. J.; Berka, V.; Babcock, T. G.; Tsai, A. *Biochemistry* **2002**, *18*, 5695.

(22) Limmer, W.; Ritter, W.; Sauer, R.; Mensching, B.; Liu, C.; Rauschenbach, B. *Appl. Phys. Lett.* **1998**, *72*, 2589.

(23) Saitoh, H.; Utsumi, W.; Kaneko, H.; Aoki, K. *J. Cryst. Growth* **2007**, *300*, 26.

(24) Lei, L.; He, D.; He, K.; Qin, J.; Wang, S. *J. Solid State Chem.* **2009**, *182*, 3041.